Immobilization of Simulated High Level Nuclear Wastes with Li_2O-CeO_2-Fe_2O_3-P_2O_5 Glasses

Toshinori Okura, Naoya Yoshida

Abstract—The leaching behavior and structure of Li_2O-CeO_2-Fe_2O_3-P_2O_5 glasses incorporated with simulated high level nuclear wastes (HLW) were studied. The leach rates of gross and each constituent element were determined from the total weight loss of the specimen and the leachate analyses by inductively coupled argon plasma spectroscopy (ICP). The gross leach rate of the 4.5Li_2O-9.7CeO_2-34.7Fe_2O_3-51.5P_2O_5 glass waste form containing 45 mass% simulated HLW is of the order of 10^{-5} g/cm^2·day at 90˚C, which is nearly equal as compared with the corresponding release from a currently used borosilicate glass waste form. The isolated ions such as monomeric $(PO_4)^{3-}$ ions increase upon as increasing the incorporating amount of the simulated HLW. The changes in properties can be attributed to the structure changes owing to the incorporation of the simulated HLW. It was found that the Li_2O-CeO_2-Fe_2O_3-P_2O_5 glass works well as a matrix to solidify HLW.

Keywords—FT-IR spectra, Leach rates, Li_2O-CeO_2-Fe_2O_3-P_2O_5 glasses, Nuclear waste immobilization, Thermal properties

I. INTRODUCTION

THE disposal of radioactive waste generated by the nuclear fuel cycle is among the most pressing and potentially costly environmental problems. The high level nuclear wastes (HLW) are immobilized in a stable solid state and completely isolated from the biosphere.

Nuclear waste glasses are typically borosilicate glasses, and these glass compositions can experience phase separation at elevated concentrations of P_2O_5. The maximum P_2O_5 concentrations must be limited to between 1 and 3 mass%. For some waste streams, this can require considerable dilution and a substantial increase in the volume of the waste glass produced. Hence, there has been a continuing interest in developing phosphate glasses as waste forms. Further, typical borosilicate glasses are limited to no more than 5 mass% actinides (2 mass% for Plutonium). In contrast iron phosphate glass with up to 15 mass% P_2O_5 can accommodate up to 40 mass% of simulated HLW [1], [2].

The atomic bonding characteristics of phosphate glasses in many respects more closely resemble organic polymers than silicate networks, and this leads to many differences in properties between the two families of glasses. In general, phosphate based glasses are less stable thermally than their silicate equivalents and they are considerably less durable, particularly in aqueous environments, although there are some notable exceptions.

Toshinori Okura is with the Department of Environmental and Energy Chemistry, Faculty of Engineering, Kogakuin University, 2665-1, Nakano, Hachioji, Tokyo 192-0015, Japan (phone and fax: +81-42-628-4149; e-mail: okura@cc.kogakuin.ac.jp).

Naoya Yoshida is with the Department of Environmental and Energy Chemistry, Faculty of Engineering, Kogakuin University, 2665-1, Nakano, Hachioji, Tokyo 192-0015, Japan (e-mail: nyoshida@cc.kogakuin.ac.jp).

Phosphate glasses have some advantages over borosilicate glasses, such as lower melting temperatures, lower melt viscosities and higher solubility for problematic elements, such as sulfur, and were investigated as early as the 1960s. Later work on sodium-aluminum phosphate glass [3] and iron-aluminum phosphate glass [4] showed that some of these glasses had comparable or better chemical durability than the borosilicate glasses. Present efforts are focused on the development of lead-iron phosphate glasses [1], [5]-[10]. The main disadvantage of phosphate glass is that the melts are highly corrosive. Still, a number of the engineering problems were overcome and in the 1980s at Mayak in the Urals, considerable amounts of waste, approximately 1000 m^3, were immobilized in a phosphate glass [11]. Vitrification of wastes with Na-Al phosphate glass matrix continues today at the Mayak Production Association in Chelyabinsk where 300 million Curies of activity of HLW have been immobilized in glass. There have been studies to investigate the immobilization of Cs [12], CsCl and SrF$_2$ [13], mixed-waste sludge [14] and spent nuclear fuel [2] in iron phosphate glass compositions. More recently, we have developed a new family of magnesium phosphate glasses [15]-[17]. In this study, Li_2O-CeO_2-Fe_2O_3-P_2O_5 glasses are chosen as the base glass. Mixed metal oxide, which acts as the simulated nuclear waste (radioactive isotopes were not employed) [18], was incorporated into the base glass to study its effects on the properties of the glasses. The present article reports on the leach rates to water, some of thermal properties and microstructure. The variations of the glass structure due to the incorporation of the simulated HLW are also examined by Fourier-transformed infrared (FT-IR) spectra.

II. EXPERIMENTAL PROCEDURE

A. Sample preparation

The Li_2O-CeO_2-Fe_2O_3-P_2O_5 glass frit that is used to produce glass waste form can be prepared by combining appropriate amounts of Li_2CO_3, Ce_2O_3, Fe_2O_3, and $(NH_4)HPO_3$ and by heating at 1250˚C for 1h. The powder mixtures of the glasses containing 25 and 45 mass% of simulated HLW were melted at 1250˚C for 2h. The melt waste glass was poured into a stainless plate. The composition of the simulated HLW is shown in Table I. Compositional data of phosphate glasses considered for the immobilization of simulated HLW are summarized in Table II.

B. Leach test

According to the technique of MCC-2 [19], the leach test for the glass waste forms was conducted in distilled water. About 1 g of each sample crushed to 10-20 mesh was dipped into 50 ml of water in a Teflon beaker within an oven kept at 90˚C for 20 days.

TABLE I
COMPOSITION OF SIMULATED NUCLEAR WASTES

Waste element	Raw material	mass%
Na	$NaNO_3$	64.8
Sr	SrO	2.9
La	La_2O_3	16.1
Mo	MoO_3	7.5
Mn	MnO_2	1.2
Fe	Fe_2O_3	6.6
Te	TeO_2	0.9

The total surface area of the grains was estimated by the following:

$$S = W S_0 / \rho \tag{1}$$

where W and ρ are the mass in g and the density in g/cm^3 of sample, and S_0 the specific surface of crushed specimen, respectively. The leach rates of gross and each constituent were determined from the total weight loss of the specimen and the leachate analyses by inductively coupled argon plasma spectroscopy (ICP).

C. XRD, DTA, SEM and FT-IR spectra

Powder X-ray diffraction (XRD) analysis of the as-quenched melt was used to verify the amorphous state of the samples. The differential thermal analyses (DTA) were performed in flowing nitrogen at a heating rate of 10°C/min. The microstructure of the waste forms was investigated with the scanning electron microscope (SEM). The FT-IR spectra were measured using the KBr pellet technique in the frequency range 400-2000 cm^{-1} at room temperature.

III. RESULTS AND DISCUSSIONS

A. Vitrification of Li_2O-CeO_2-Fe_2O_3-P_2O_5 waste glasses

To understand the effect of temperature on the crystallization of Li_2O-CeO_2-Fe_2O_3-P_2O_5 waste glasses, the samples were annealed isothermally at 500°C for 10h. The glass states were confirmed by the absence of XRD peaks.

The results of XRD measurement are shown in Table III. The glass forming tendency increased with the decreasing F/P ratio, and up to 45 mass% loadings of the simulated HLW can be incorporated into the base Li_2O-CeO_2-Fe_2O_3-P_2O_5 glasses.

TABLE II
COMPOSITION OF GLASS WASTE FORMS PREPARED IN THIS STUDY

Glass system	Waste Content (mass%)	Fe_2O_3:P_2O_5=40:60 (mass ratio)	Fe_2O_3:P_2O_5=30:70 (mass ratio)
Fe_2O_3-P_2O_5	0	40F60P 0W	30F70P 0W
Li_2O-Fe_2O_3-P_2O_5	0	10L36F54P 0W	10L27F63P 0W
CeO_2-Fe_2O_3-P_2O_5	0	10C36F54P 0W	10C27F63P 0W
Li_2O-CeO_2-Fe_2O_3-P_2O_5	0	4.5L9.7C34.3F51.5P 0W	4.5L9.7C25.7F60.1P 0W
	25	4.5L9.7C34.3F51.5P25W	4.5L9.7C25.7F60.1P25W
	45	4.5L9.7C34.3F51.5P45W	4.5L9.7C25.7F60.1P45W

L: Li_2O C:CeO_2 F:Fe_2O_3 P:P_2O_5 W:Waste

TABLE III
THE RESULTS OF XRD MEASUREMENT

Glass waste forms	Vitreous state; V or Crystalline state; C	
	Before heat-treatment	After heat-treatment at 500°C for 10h
4.5L9.7C34.3F51.5P 0W	V	C
4.5L9.7C34.3F51.5P25W	V	C
4.5L9.7C34.3F51.5P45W	V	C
4.5L9.7C25.7F60.1P 0W	V	V
4.5L9.7C25.7F60.1P25W	V	V
4.5L9.7C25.7F60.1P45W	V	V

TABLE IV
LEACH RATE OF EACH CONSTITUENT ELEMENT OF GLASS WASTE FORMS
(A) $Li_2O : CeO_2 : Fe_2O_3 : P_2O_5 = 4.5 : 9.7 : 34.3 : 51.5$
($Fe_2O_3 : P_2O_5 = 40 : 60$) Leach rate; g/cm²·day

Waste (mass%)	10	25	45
Gross	5.59×10^{-5}	3.81×10^{-5}	3.28×10^{-5}
P	1.22×10^{-5}	9.36×10^{-5}	4.45×10^{-6}
Fe	1.09×10^{-6}	3.19×10^{-6}	2.18×10^{-7}
Ce	3.47×10^{-7}	1.45×10^{-7}	1.72×10^{-10}
Li	2.10×10^{-6}	1.89×10^{-6}	1.19×10^{-5}
Na	3.14×10^{-6}	4.15×10^{-6}	5.17×10^{-7}
Sr	5.24×10^{-6}	1.27×10^{-7}	6.89×10^{-8}
La	1.75×10^{-8}	9.07×10^{-8}	3.45×10^{-9}
Mo	1.75×10^{-7}	1.12×10^{-6}	6.89×10^{-7}
Te	n.d.	3.63×10^{-8}	n.d.

(B) $Li_2O : CeO_2 : Fe_2O_3 : P_2O_5 = 4.5 : 9.7 : 25.7 : 60.1$
($Fe_2O_3 : P_2O_5 = 30 : 70$) Leach rate; g/cm²·day

Waste (mass%)	10	25	45
Gross	2.27×10^{-4}	1.14×10^{-4}	1.36×10^{-4}
P	3.88×10^{-6}	2.25×10^{-7}	4.53×10^{-7}
Fe	7.08×10^{-7}	6.62×10^{-7}	6.29×10^{-7}
Ce	1.57×10^{-6}	2.14×10^{-7}	n.d.
Li	n.d.	n.d.	n.d.
Na	n.d.	n.d.	n.d.
Sr	n.d.	n.d.	n.d.
La	n.d.	n.d	n.d.
Mo	n.d.	n.d.	n.d.
Te	n.d.	n.d.	1.34×10^{-5}

It was found that the 4.5L9.7C25.7F60.1P was thermally stable form. The borosilicate glasses are limited to no more than 5 mass% actinides. In contrast Li_2O-CeO_2-Fe_2O_3-P_2O_5 glasses can accommodate up to 45 mass% of simulated HLW.

B. Leach rates of samples in water

The gross leach rates and the leach rates of each constituent element of the sample in water at 90˚C were determined from the total weight loss of the specimen and chemical analysis of leachate solution. The results are summarized in Table IV. The 4.5L9.7C34.3F51.5P waste form has the gross leach rate of the order of 10^{-5} g/cm²·day, which is nearly equal as compared with that of the borosilicate waste glass. The chemical durability of the glasses was improved as the addition of simulated HLW. Up to 45 mass% loadings of the simulated HLW can be incorporated into the base glasses. Of the elements in most phosphate glasses, Na shows higher leach rate than others, probably because of rather higher solubility of its polyphosphate consisting of chains of phosphate ions. No effect of Na in the Li_2O-CeO_2-Fe_2O_3-P_2O_5 glass waste form on its leachability was found. The 4.5L9.7C25.7F60.1P waste form has the gloss leach rate of the order of 10^{-4} g/cm²·day, which is high as compared with that of the borosilicate waste glass. However, the leach rates of each constituent element of the simulated HLW were fairly low as compared with that of the base glasses.

C. Thermal properties of glass waste form

It is important to obtain information about the thermal stability of the glass waste form, since the crystallization of glass waste can mostly increase the undesirable aqueous corrosion rate of the form, probably due to the formation of somewhat more soluble crystals or the increase in surface area.

Table V shows the glass transition temperatures (Tg) and the starting temperatures of crystallization (Tc) determined by DTA curves of the samples and the stability of the waste forms (Tc-Tg) are shown in Fig. 1.

TABLE V
THE RESULTS OF DTA MEASUREMENT OF GLASS WASTE FORMS

Glass waste forms	40F60P	10L36F54P	10C36F54P	4.5L9.7C34.3F51.5P		
Waste	0W	0W	0W	0W	25W	45W
Tg (ºC)	542	454	530	506	499	446
Tc (ºC)	791	502	542	599	573	525

Glass waste forms	30F70P	10L27F63P	10C27F63P	4.5L9.7C25.7F60.1P		
Waste	0W	0W	0W	0W	25W	45W
Tg (ºC)	518	552	559	490	497	481
Tc (ºC)	723	718	743	657	518	540

Tg ; glass transition temperature   Tc ; starting temperature of crystallization

It indicates that both Tc and Tg decrease with increasing simu lated HLW content. The glass waste forms containing 45 mass % simulated HLW were thermally stable.

D. Microstructure

Figs. 2 and 3 show the SEM photographs for the 4.5L9.7C34.3F51.5P and 4.5L9.7C25.7F60.1P glass waste forms, respectively, before and after leaching with simulated waste content of 25 and 45 mass%. All samples before leaching were vitreous states. This fact corresponds to the results of XRD measurements. In the samples after leaching, the precipitates were observed uniformly.

E. FT-IR spectra of glass waste form

The results of FT-IR measurements of the glass waste forms are shown in Fig. 4 and Table VI. The band near 1300 cm^{-1} is attributed to (P=O) stretching mode. The band becomes smaller indicating a decrease in the double bond character and in the effective force constant of the (P-O) bond as found in ultraphosphates with increasing the simulated HLW content.

The band near 1200 cm^{-1} is assigned to asymmetric stretching modes of the two non-bridging oxygen atoms bonded to phosphorus atoms, $(PO_2)_{asym}$ or Q^2 units, in the phosphate tetrahedra. Their amplitudes increase with increasing waste content. This result indicates that the phosphate linkages are shortened as the simulated HLW incorporate into the glass structure and leading to decrease the relative content of the Q^2 units.
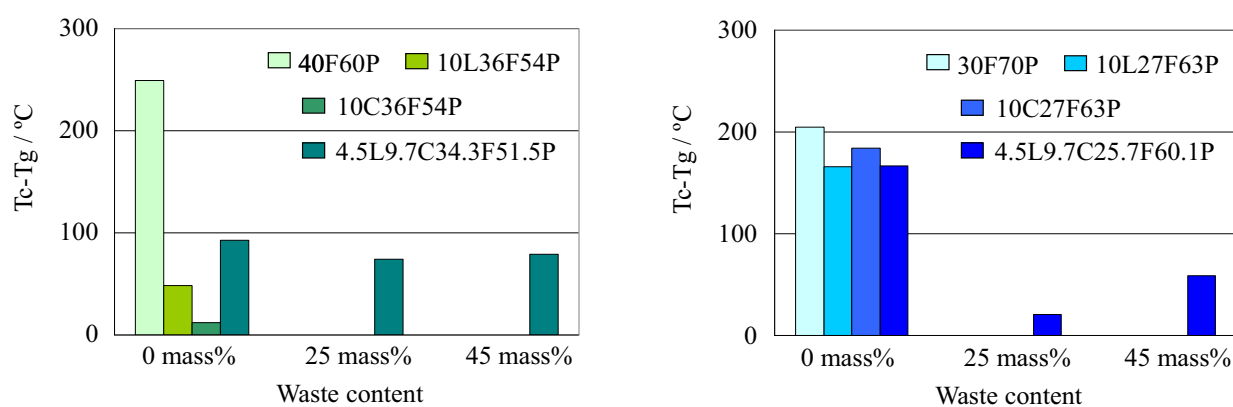

Fig. 1 The stability of glass waste forms

4.5L9.7C34.3F51.5P 0W
before leaching

4.5L9.7C34.3F51.5P25W
before leaching

4.5L9.7C34.3F51.5P45W
before leaching

4.5L9.7C34.3F51.5P 0W
after leaching

4.5L9.7C34.3F51.5P25W
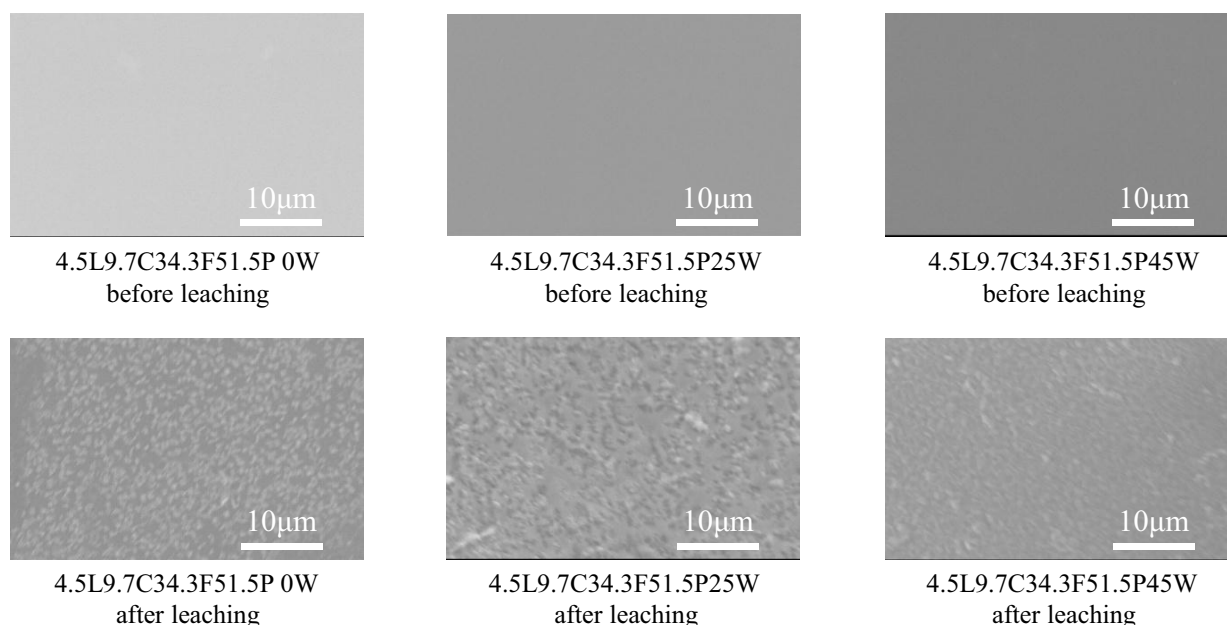after leaching

4.5L9.7C34.3F51.5P45W
after leaching

Fig. 2 SEM photographs of 4.5L9.7C34.3F51.5P glass waste forms
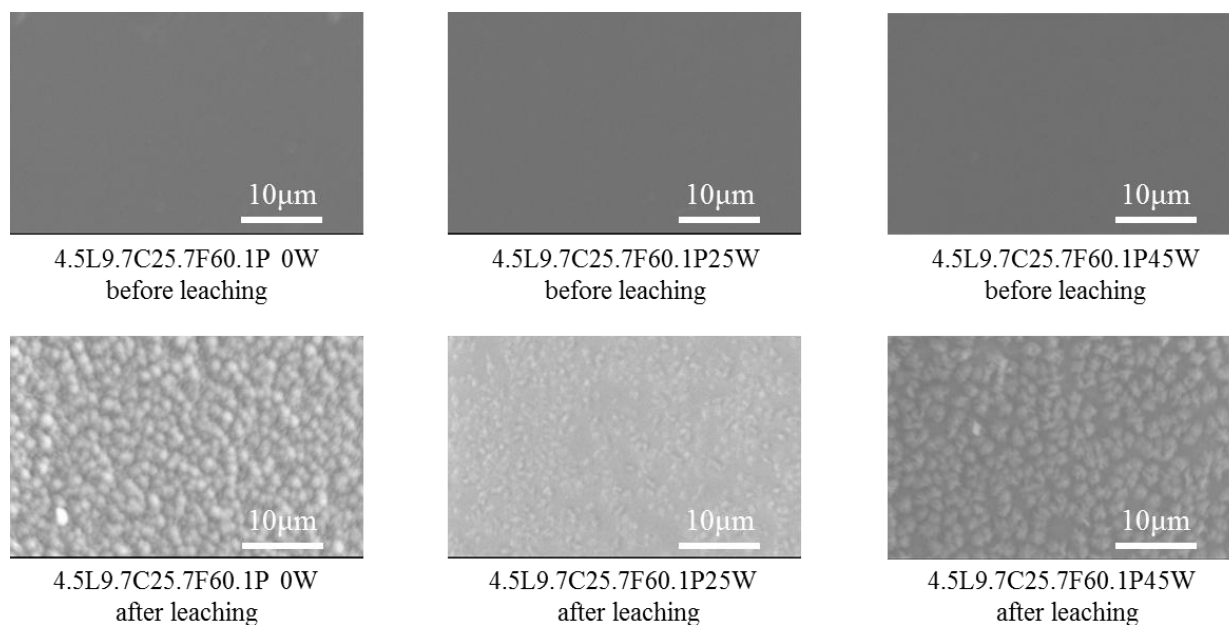
Fig. 3 SEM photographs of 4.5L9.7C25.7F60.1P glass waste forms

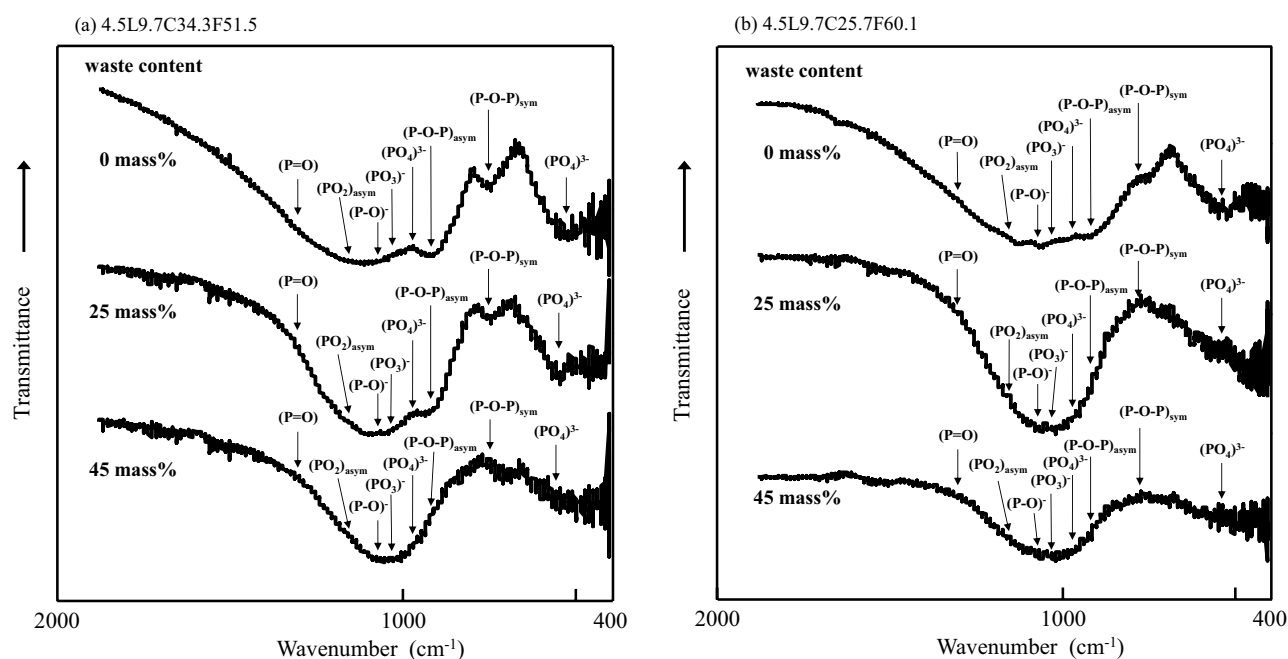Fig. 4 FT-IR spectra of the glass waste forms

The absorption bands near 1100 cm^{-1} have been assigned to (P-O)$^{-}$ groups, and its amplitudes increase with increasing waste content. It is suggested that the absorption bands of (R-O-P) (R = waste element) also locate at near 1100 cm^{-1}, and the relative content of these bonds increase with increasing waste content leading to increased intensity of 1100 cm^{-1} band.

The intensity of the band near 1050 cm^{-1}, which is assigned to (PO$_3$) end groups (Q^1), tends to increase with increasing waste content. The absorption bands near 980 cm^{-1} and 420-500 cm^{-1} are assigned to the stretching and deformation modes of (PO$_4$)$^{3-}$ groups (Q^0), respectively. It is shown that the absorption bands of the deformation modes of (PO$_4$)$^{3-}$ group shift to higher frequencies, and the amplitudes of (PO$_4$)$^{3-}$ group's absorption bands near 980 cm^{-1} increase with increasing waste content. The

TABLE VI
THE RESULTS OF FT-IR MEASUREMENT OF GLASS WASTE FORMS

Wave number (cm^{-1})	1300	1200	1100	1050	980	900	700	420-500
	(P=O)	$(PO_2)_{asym}$	$(P-O)^-$	$(PO_3)^-$	$(PO_4)^{3-}$	$(P-O-P)_{asym}$	$(P-O-P)_{sym}$	$(PO_4)^{3-}$
	decrease	increase	increase	increase	increase	decrease	decrease	shift*

＊; shift to higher frequency

Q^1 and Q^0 groups increase with increasing waste content. These results indicate that the relative content of non-bridging oxygen $(P-O^-)$, which may be replaced by the formation of (R-O-P) bonds, increases as the incorporation of the simulated HLW.

The absorption bands near 900 and 700 cm^{-1} are assigned to the asymmetric and symmetric stretching modes of the (P-O-P) linkages, respectively. Their amplitudes obviously decrease with increasing waste content. The phosphate linkages of the glasses with higher waste content are shorter due to the depolymerization of the glass structure.

The formation of asymmetric bridging oxygen (R-O-P) would increase the cross-link density of the glass network, improving the chemical durability of the glasses.

IV. CONCLUSION

$Li_2O-CeO_2-Fe_2O_3-P_2O_5$ glasses were proposed as the potential nuclear waste glasses. The leach rates, some thermal properties and structure of the glasses loaded with simulated HLW were examined. The main features of this work are as follows:

(1) Up to 45 mass% loadings of the simulated HLW can be incorporated into the base $Li_2O-CeO_2-Fe_2O_3-P_2O_5$ glasses. The glass waste forms containing 45 mass% simulated HLW were vitreous states and thermally stable. The chemical durability of the glasses was improved as the addition of simulated HLW.
(2) The leach rate of the waste glasses decreases with increasing the simulated HLW content. The gross leach rate of the 4.5L9.7C34.3F51.5P waste form is of the order of 10^{-5} g/cm^2·day at 90˚C, which is nearly equal as compared with that of the borosilicate waste glass.
(3) With increasing waste content, the band characteristic of the orthophosphate monomer $(PO_4)^{3-}$ species increased.
(4) The formation of asymmetric bridging oxygen (R-O-P) increases the cross-link density of the glass network, improving the chemical durability of the glasses.

ACKNOWLEDGMENT

REFERENCES

[1] D. E. Day, Z. Wu, C. S. Ray and P. Hrma. *J. Non-Cryst. Solids*, 241, 1-12 (1998).
[2] M. G. Mesko and D. E. Day, *J. Nucl. Mater.*, 273, 27-36 (1999).
[3] J. Van Geel, H. Eschrich, W. Heimerl and P. Grziwa, *IAEA*, *Vienna*, 22-26 (1976).
[4] B. Grambow and W. Lutze, "Scientific Basis for Nuclear Waste Management, Vol. 2. Northrup", ed. by CJM, Jr, Plenum Press, New York (1979) pp. 109-116.
[5] B. C. Sales and L. A. Boatner, *Science*, 226, 45-48 (1984).
[6] B. C. Sales and L. A. Boatner, "Radioactive Waste Forms for the Future", ed. by W. Lutze and R. C. Ewing, North-Holland, Amsterdam (1988) pp. 193-231.
[7] T. Yanagi, M. Yoshizoe and N. Nakatsuka, *J. Nucl. Sci. Technol.*, 25, 661-6 (1988).
[8] T. Yanagi, M. Yoshizoe and K. Kuramoto, *J. Nucl. Sci. Technol.*, 26, 948-54 (1989).
[9] S. T. Reis, M. Karabulut and D. E. Day, *J. Nucl. Mater.*, 304, 87-95 (2002).
[10] P. Y. Shin, *Mater. Chem. Phys.*, 80, 299-304 (2003).
[11] W. Lutze, "Radioactive Waste Forms for the Future", ed. by W. Lutze and R. C. Ewing, North-Holland, Amsterdam (1988) pp. 1-159.
[12] S. T. Reis and J. R. Martinelli, *J. Non-Cryst. Solids*, 247, 241-7 (1998).
[13] M. G. Mesko, D. E. Day and B. C. Bunker, *Waste Management*, 20, 271-278 (2000).
[14] R. D. Spence, T. M. Gilliam, C. H. Mattus and A. J. Mattus, *Waste Management*, 19, 453-65 (1999).
[15] T. Okura, T. Miyachi and H. Monma, *Trans. Mater. Res. Soc. Jpn.*, 29[5], 2175-2178 (2004).
[16] T. Okura, T. Miyachi and H. Monma, *J. Eur. Ceram. Soc.*, 26/4-5, 831-836 (2006).
[17] T. Okura, K. Yamashita and T. Kanazawa, *Phys. Chem. Glasses*, 29, 13-17 (1988).
[18] M. Ishida, T. Yanagi and R. Terai, *J. Nucl. Sci. Technol.*, 24, 404-408 (1987).
[19] D. M. Strachan, "Scientific basis for nuclear waste management", ed. by J. D. Moor., Plenum Press, New York (1980) pp. 347-348.